



In Silico Analysis of S315T and S315R Mutations of Multidrug-resistant *Mycobacterium tuberculosis* Clinical Isolates from Karachi, Pakistan

Muhammad Mumtaz Khan¹, Maria S Alves², Sadia Alam^{1*}, Mohammad H Khan³, Muhammad Jahangir⁴, Abdul Jabbar⁵, Rehmat Zaman⁶, Sajid Ali⁷, Aisha Bibi¹ and Mustafa Kamal⁸

¹Department of Microbiology, The University of Haripur, Haripur, Pakistan

²Department of Pharmaceutical Sciences, Faculty of Pharmacy, Federal University of Juiz de Fora, Minas Gerais, Brazil

³Department of Health Sciences, City University of Science and Technology, Peshawar, Pakistan

⁴ Department of Food Science and technology, The University of Haripur, Haripur, Pakistan

⁵Department of Medical Lab technology, The University of Haripur, Haripur, Pakistan

⁶Business Incubation Center, The University of Haripur, Haripur, Pakistan

⁷Provincial Reference Lab of Tuberculosis, Peshawar, Pakistan

⁸Department of Biotechnology, University of Karachi, Karachi, Pakistan

*Corresponding author: Department of Microbiology, University of Haripur, Haripur, Pakistan. Email: sadia.alam2004@gmail.com

Received 2020 February 10; Revised 2020 November 04; Accepted 2020 November 08.

Abstract

Background: Tuberculosis is one of the most frequent and persistent global diseases causing millions of deaths every year. Pakistan lies at number 6 among the 22 most dominant countries, with multidrug resistance up to 15%. Isoniazid-resistant strains of *Mycobacterium tuberculosis* are gradually rising and seem to be more prevalent in developing countries. Mutations in the *katG* gene are considered to be responsible for the accusation of isoniazid resistance in *M. tuberculosis*.

Objectives: The current study was designed to investigate the structural and functional associations of *KatG* gene mutations (S315R and S315T) and multidrug resistance in *M. tuberculosis* isolates from Karachi, Pakistan.

Results: The present study revealed conformational changes in the structure of the *KatG* enzyme due to observed mutations, which led to induced alterations in isoniazid binding residues at the active site of the *KatG* enzyme. Furthermore, substantial changes were observed in interaction energy, ligand-receptor energy, electrostatic energy, salvation energy, and ligand-receptor conformational entropy. All these resultant modifications due to S315R and S315T mutations ultimately reduced the flexibility and stability of proteins at isoniazid-binding residues.

Conclusions: This deviation in the consistency of protein texture eventually compromises the enzyme activity. It is well expected that the outcomes of the current study would provide a better understanding of the consequences of these mutations and provide a detailed insight into some previously unknown features.

Keywords: *Mycobacterium tuberculosis*, *KatG*, Isoniazid, Resistance, Mutation, Docking

1. Background

Tuberculosis is an airborne disease, primarily caused by *Mycobacterium tuberculosis* (MTB), affecting vital parts of the body, including the lungs, central nervous system, and lymphatic system (1, 2). According to an estimate, the overall incidence of tuberculosis is reported to be 10 million, accounting for 9.6 - 13.3 million cases in 2018. Moreover, in 2018, the alarming incidence of Multidrug Resistance (MDR) were was 186, 772 cases, and 1.2 million deaths worldwide (3). The risk factors that influence tuberculosis are HIV, diabetes, smoking, alcoholism, and malnutrition (3).

Multidrug-resistant strains mainly emerge due to the development of resistance against the most important and

commonly used anti-tuberculosis drugs like rifampicin and isoniazid (4, 5) and contribute mainly to the persistence of relevant infections worldwide (6, 7). Resistance against isoniazid (INH), one of the most effective anti-tuberculosis drugs due to its fastidious potency, is due to genetic aberrations in codons of the hyper-variable region of the *katG* gene (4). It is also well documented that these mutations usually result in the loss of catalase-peroxidase activity (8, 9), with the majority of them happening in codon 315. However, 30% to 90% of the isoniazid-resistant isolates are associated with the geographical distribution of the population (10).

Isoniazid is one of the drugs inhibiting the biosynthesis of cell wall mycolic acid (long-chain α -branched β -

hydroxylated fatty acids) and hence, makes MTB susceptible to oxygen radicals (11). The INH prodrug mostly targets InhA (enoyl-ACP reductase), but it needs activation by the catalase-peroxidase enzyme coded by the *katG* gene to form reactive free radicals, which then bind covalently to NAD⁺ to make the isonicotinoyl-NAD complex (12, 13). This complex then binds strongly to the active site of the inhA enzyme, which is actually NADH-dependent enoyl-acyl carrier protein (ACP) reductase and leads to overcrowding of the natural enoyl-AcpM substrate and thus inhibits the biosynthesis of both fatty acids and mycolic acid.

The intrinsic resistance of MTB to hydrophilic antibiotics is believed to be due to the formation of porins in low efficiency in synergy with other resistance mechanisms like enzymatic inactivation or active efflux of drugs. The only peroxide inducible to MTB is *KatG*, which uses one molecule of hydrogen peroxide (H₂O₂) as a substrate. However, other molecules of H₂O₂ act as oxidants and result in the destruction of this toxic substance and lead to the formation of water and oxygen molecules. It has been revealed that catalase activity is essential for the survival of MTB in highly oxidizing environments. The catalytic activity of *KatG* is mainly due to its structural features, i.e., Met-Tyr-Trp, a covalent cross-link; however, the mutated *KatG* gene lacks this distinct structural feature (14). Molecular docking can reveal these mutations in the tuberculosis pathogen and may be responsible for drug resistance in isolates from Karachi, Pakistan.

2. Objectives

This study was carried out to analyze the S315R and S315T mutations in MDR-MTB strains of sputum samples concerning their effects on the structure, function, and binding affinity and to determine the extent to which they affect the respective protein. This study is expected to be helpful in the further understanding of the consequences posed by these point mutations and the potential molecular causes of this threatening disease. It will also guide further studies towards the development of better treatment strategies against the havoc posed by different diseases, including tuberculosis. The detailed investigations will also provide valuable insight into some of the features that have not been previously studied.

3. Methods

3.1. Sample Collection

Sputum samples were collected from pulmonary tuberculosis patients at the Ojha Institute of Chest Diseases (OICD), Dow University of Health Sciences, Karachi, Pakistan, after obtaining patients' consent.

3.2. Staining and Culture

Decontamination of sputum samples was done by using the N-acetyl-L-cysteine sodium hydroxide (NALC-NaOH) concentrated method (15), where NaOH was used as the decontaminating agent and NALC as the mucolytic agent. Sodium citrate attaches to heavy metal ions, which might be present in the samples because these ions attach to NALC and then inactivate it. Sputum and NALC-NaOH samples were then transferred to falcon tubes of up to 5 mL. Next, an equal volume of NALC-NaOH was added to the tubes. Screw caps were tightened, and the tubes were vortexed for 20 s. The tubes were then incubated for 15 min at room temperature and allowed to be decontaminated.

Furthermore, phosphate buffer was added to falcon tubes up to 50 mL and then vortexed, followed by centrifugation for 15 min at 3,000 rpm. The supernatant was poured off by using a funnel into a discordant containing 5% phenol or other mycobacterial disinfectants. A phosphate buffer solution of 0.3 mL was added to sediments to re-suspend them. The sediment of the processed specimen was inoculated into Lowenstein Jenson (LJ) medium using a sterilized pipette, and slides were prepared for Ziehl-Neelsen (ZN) staining. Microscopy was done for the presence of acid-fast bacteria. The media were incubated at 37°C for up to eight weeks or the appearance of any visible colonies, whichever was earlier. After incubation, if cultures yielded no growth, they were declared as negative. Otherwise, they were considered for DNA isolation and further processing.

3.3. DNA Extraction and PCR Amplification

Three to five colonies from solid LJ medium were suspended in 1 mL of molecular biology grade sterile distilled water and were incubated at 95°C for 30 min, followed by 15 min placement in an ultrasonic bath. Tubes containing *M. tuberculosis* were centrifuged at 13,000 rpm for 10 min at 4°C. The supernatant was taken and was transferred to a new tube. Then, 2 µL of this supernatant was used for PCR analysis (4). The 210 bp segment of the *katG* gene, a hyper-variable isoniazid resistance region, was amplified using the following synthetic oligonucleotide primers: 5'-GAAACAGCGCGCTGGATCGT-3' and 5'-GTTGTCCCATTTTCGTCGGGG-3' (16, 17).

The PCR amplification was done at 94 °C for 10 min for initial denaturation, followed by 40 cycles at 94 °C for one minute, annealing at 45 °C for one minute, extension at 72 °C for one minute, and a final extension at 72 °C for seven minutes, in sequence. For visual analysis, gel electrophoresis was performed on the amplified PCR products. To this end, 5 µL of the PCR product was separated through the 2% agarose gel in horizontal gel electrophoresis by supplying

an electric voltage of 80 volts. Furthermore, gel staining was done using ethidium bromide (0.5 $\mu\text{g}/\text{mL}$), visualized by UV, and then photographed (3).

3.4. PCR Product Sequencing

As known, PCR-DNA sequencing is a straightforward technology to detect a mutation. For the sequencing purpose, the amplicon was sent to Macrogen Inc., South Korea. The DNA sequencing data were analyzed by comparing with the H₃₇Rv reference strain through the NCBI blast (18-20).

3.5. Datasets

The crystal structure of wild-type MTB with PDB ID:1SJ2 was retrieved from the RCSB Protein Data Bank as a reference. Mutant models of the *KatG* protein were generated through the mutate model, an application of the modeler available as a python script (21). The optimization of all the predicted models was done using the CHARMM force field while several servers like WHAT IF, ProSA-web, and APOLLO were used for validations (22). The 3D structure of isoniazid was retrieved from PubChem, a database maintained in NCBI (23).

3.6. Docking of Wild-type and Mutated *KatG* with Isoniazid

Dozens of effective automated docking methods are available for the prediction of biomolecular complexes in structural and functional analyses. AutoDock provides an efficient prediction of bound conformations through a combination of the Lamarckian Genetic Algorithm and an empirical free energy force field. Wild-type and mutant *KatG* proteins of MTB were, therefore, docked to INH using AutoDock4 (16, 17), a newer version of AutoDock, that integrates the explicit conformational modeling of specified side chains in the receptor and also provides an effective way to analyze the covalently attached ligands. The docked complexes were examined to investigate the potential variations in hydrogen bonding and other interactions. Wild conformations, torsions, and direction of the ligand molecules were set at random. Each docking experiment was derived from 10 different runs that were set to terminate after a maximum of 250,000 energy evaluations. The population size was kept at 150, while a translational step of 0.2 $^{\circ}\text{A}$ and quaternion and torsion steps of five were applied throughout the search.

4. Results

4.1. Molecular Analysis

The MDR clinical isolates of patients from Karachi, Pakistan, were found to be resistant to prodrug isoniazid after culturing and susceptibility testing. Strains resistant to

isoniazid were screened and further processed to study at a molecular level. The 210 bp covering the hot spot region of the *katG* gene was amplified via the Nested PCR technique and further examined by gel-electrophoresis (Figure 1).



Figure 1. The 210 bp fragment of the amplified product displaying a positive band when exposed to UV light after gel electrophoresis; 1-3 represent the clinical isolates of *Mycobacterium tuberculosis*.

4.2. Sequence Analysis

Our investigation revealed mutations to confer isoniazid resistance in clinical isolates, and the examined strains from tuberculosis patients were resistant to the isoniazid prodrug. The 210 bp amplified region of the *katG* gene covered the hotspot region. The sequencing results of the isoniazid-resistant strains covering codon 315 showed two mutations when comparative BLAST and multiple alignments were run by the online CLUSTAL W2 tool. Two different mutations were observed at codon 315: AGC \rightarrow ACC (Ser \rightarrow Thr) and AGC \rightarrow CGC (Ser \rightarrow Arg) (Figure 2). Due to these mutations, prodrug isoniazid might not be activated due to improper binding to the catalase-peroxidase enzyme, responsible for drug activation. Our subsequent analysis in isoniazid-resistant isolates was a significant addition to previous studies. This analysis may play an important role in recognizing the isoniazid resistance event. The new alleles found in this study were suc-

cessfully submitted to DDBJ (NCBI/GenBank) under accession numbers AB776022 and AB776695.

4.3. Structure Analysis

The position of the mutation at codon 315 was analyzed in the ribbon structure of the *KatG* protein. The protein is colored grey, while the side chain of the mutated residue is colored magenta and shown as small balls. This shows the position of the mutation in the ribbon structure (Figure 3). Our structural analysis further envisages that mutations Serine to Threonine and Serine to Arginine at codon 315 differ in many aspects, especially size and hydrophobic properties. We found that the mutant residue was bigger than the wild one, while mutant residues were comparatively less hydrophobic and bear positive charges, as shown in Figures 4 and 5.

4.4. Docking Studies with Isoniazid Prodrug

Docking studies were performed through the computational investigation of the docking score and interaction energy between ligand (isoniazid) and MTB KTG protein (1SJ2) retrieved from the protein data bank. AutoDock4 was used for protein-ligand docking, which is an automated molecular docking software package (16). The ligand-protein interaction energies were computed via the PEARLS Program (24), an online resource for energetic analysis of the receptor-ligand system. It computes the total ligand-receptor interaction, electrostatic van der Waals, hydrogen bonds, and solvation free energies along with the ligand-receptor conformational entropy, as shown in Figures 5 and 6. These are physically significant representations of molecules perceived by another molecule in its locality. The negative value of electrostatic energy increased the interaction and vice versa, as shown in Table 1. We observed variations in the bonding patterns of key binding residues of the mutant *KatG* protein and wild-type *KatG* (1SJ2). The imprecise bonding pattern of mutated *KatG* with isoniazid might be responsible for resistance to isoniazid in MTB-tuberculosis strains.

5. Discussion

Isoniazid is a prodrug used as a first-line tuberculosis drug. Different studies have described different mechanisms for isoniazid resistance and have reported multiple mutations in different genes. Different studies have reported that about 50 to 84% of resistance against isoniazid is due to one mutation in *ktG* whereas 10 - 35% of resistance is due to at least one mutation in the *inhA* promoter, and 10 to 40% of resistance is due to at least one mutation in *oxyR-ahpC* (Li et al., 2015). Mutations at *katG* lead to a high level

of isoniazid resistance (25). In our wet-lab study, clinical isolates from the Ojha Institute of Chest Disease, Karachi, Pakistan, were examined, and their susceptibility patterns were investigated. We revealed two important mutations, namely S315T and S315R, in *KatG* (Figure 2).

A comprehensive investigation about the molecular modeling and dynamics of isoniazid binding with *KatG* would be helpful for the improvement of therapeutics and can be used against other complex disorders. This study was systematically designed to explore the three-dimensional spatial arrangements and conformational changes at a significant residue contributing to INH binding due to arginine and threonine substitutions. It was observed that the wild-type residue (Serine 315) had interactions with a ligand annotated as heme but significant dissimilarities in the properties of mutant *KatG* enzyme residues resulted in the loss of the binding affinity to the ligand.

The wild-type residue (Serine) forms a hydrogen bond with isoleucine at position 317, which can be disrupted by the change in the size of wild and mutant-type residues due to the positional changes introduced by mutant residues to make the same hydrogen bond. The mutation is located in a domain primarily important for protein activity and contact with another domain. These interactions could also be disturbed by mutations, which may negatively affect the protein functions including signal transduction between the domains.

There are also differences in charges between the wild and mutant-type residues. The mutants introduce a charge in a buried residue, which is at the core of the protein or protein-complex and potentially would lead to protein folding problems (26). Heme acts as a co-factor in the activation of INH. It was detected that wild-type 1SJ2 Ser315 forms two hydrogen bonds with heme having bond lengths of 2.55 Å and 2.93 Å, and one covalent bond between His270 and Fe, due to mutation S315R, it makes only a single hydrogen bond with the heme molecule with a bond length of 2.93 Å and a covalent bond with His270 and Fe. Variations in the hydrogen bond lengths of 2.91 Å and 3.24 Å were observed in the S315T mutation as compared to the wild type (Figure 5), which may cause inactivation of INH.

Protein-ligand interactions are always of prime importance in biological processes and provide an opportunity to enhance our understanding of protein function and therapeutic interventions (27). Docking calculation described the extent of the interaction of the ligand with the *KatG* enzyme and the behavior of the ligand-protein complex, as well. In the wild type (1SJ2), the ligand-receptor van der Waals energy was found to be -4.17 kcal/mol. The total ligand-receptor interaction energies of the wild type, mutant S315T, and S315R *M. tuberculosis* *KatG*-INH complex were

```

10.katG.Gene.MTB CGGCGGTCACACTTTCGGTAAGACCCATGGCGCCGGCCCGCCGATCTGGTCGGCCCCGA60
05.katG.Gene.MTB CGGCGGTCACACTTTCGGTAAGACCCATGGCGCCGGCCCGCCGATCTGGTCGGCCCCGA60
04.katG.Gene.MTB CGGCGGTCACACTTTCGGTAAGACCCATGGCGCCGGCCCGCCGATCTGGTCGGCCCCGA60
01.katG.Gene.MTB CGGCGGTCACACTTTCGGTAAGACCCATGGCGCCGGCCCGCCGATCTGGTCGGCCCCGA60
02.katG.Gene.MTB CGGCGGTCACACTTTCGGTAAGACCCATGGCGCCGGCCCGCCGATCTGGTCGGCCCCGA60
06.katG.Gene.MTB CGGCGGTCACACTTTCGGTAAGACCCATGGCGCCGGCCCGCCGATCTGGTCGGCCCCGA60
09.katG.Gene.MTB CGGCGGTCACACTTTCGGTAAGACCCATGGCGCCGGCCCGCCGATCTGGTCGGCCCCGA60
katG.gene.H37Rv CGGCGGTCACACTTTCGGTAAGACCCATGGCGCCGGCCCGCCGATCTGGTCGGCCCCGA60
03.katG.Gene.MTB CGGCGGTCACACTTTCGGTAAGACCCATGGCGCCGGCCCGCCGATCTGGTCGGCCCCGA60
08.katG.Gene.MTB CGGCGGTCACACTTTCGGTAAGACCCATGGCGCCGGCCCGCCGATCTGGTCGGCCCCGA60
*****
07.katG.Gene.MTB ACCCGAGGCTGCTCCGCTGGAGCAGATGGGCTTGGGCTGGAAGAGCTCGTATGGCACCCG120
10.katG.Gene.MTB ACCCGAGGCTGCTCCGCTGGAGCAGATGGGCTTGGGCTGGAAGAGCTCGTATGGCACCCG120
05.katG.Gene.MTB ACCCGAGGCTGCTCCGCTGGAGCAGATGGGCTTGGGCTGGAAGAGCTCGTATGGCACCCG120
04.katG.Gene.MTB ACCCGAGGCTGCTCCGCTGGAGCAGATGGGCTTGGGCTGGAAGAGCTCGTATGGCACCCG120
01.katG.Gene.MTB ACCCGAGGCTGCTCCGCTGGAGCAGATGGGCTTGGGCTGGAAGAGCTCGTATGGCACCCG120
02.katG.Gene.MTB ACCCGAGGCTGCTCCGCTGGAGCAGATGGGCTTGGGCTGGAAGAGCTCGTATGGCACCCG120
06.katG.Gene.MTB ACCCGAGGCTGCTCCGCTGGAGCAGATGGGCTTGGGCTGGAAGAGCTCGTATGGCACCCG120
09.katG.Gene.MTB ACCCGAGGCTGCTCCGCTGGAGCAGATGGGCTTGGGCTGGAAGAGCTCGTATGGCACCCG120
katG.gene.H37Rv ACCCGAGGCTGCTCCGCTGGAGCAGATGGGCTTGGGCTGGAAGAGCTCGTATGGCACCCG120
03.katG.Gene.MTB ACCCGAGGCTGCTCCGCTGGAGCAGATGGGCTTGGGCTGGAAGAGCTCGTATGGCACCCG120
08.katG.Gene.MTB ACCCGAGGCTGCTCCGCTGGAGCAGATGGGCTTGGGCTGGAAGAGCTCGTATGGCACCCG120
*****
315
07.katG.Gene.MTB AACCGGTAAGGACGCGATCACCACCGGCATCGAGGTCGTATGGACGAACACCCCGACGAA180
10.katG.Gene.MTB AACCGGTAAGGACGCGATCACCACCGGCATCGAGGTCGTATGGACGAACACCCCGACGAA180
05.katG.Gene.MTB AACCGGTAAGGACGCGATCACCACCGGCATCGAGGTCGTATGGACGAACACCCCGACGAA180
04.katG.Gene.MTB AACCGGTAAGGACGCGATCACCACCGGCATCGAGGTCGTATGGACGAACACCCCGACGAA180
01.katG.Gene.MTB AACCGGTAAGGACGCGATCACCACCGGCATCGAGGTCGTATGGACGAACACCCCGACGAA180
02.katG.Gene.MTB AACCGGTAAGGACGCGATCACCACCGGCATCGAGGTCGTATGGACGAACACCCCGACGAA180
06.katG.Gene.MTB AACCGGTAAGGACGCGATCACCACCGGCATCGAGGTCGTATGGACGAACACCCCGACGAA180
09.katG.Gene.MTB AACCGGTAAGGACGCGATCACCACCGGCATCGAGGTCGTATGGACGAACACCCCGACGAA180
katG.gene.H37Rv AACCGGTAAGGACGCGATCACCACCGGCATCGAGGTCGTATGGACGAACACCCCGACGAA180
03.katG.Gene.MTB AACCGGTAAGGACGCGATCACCACCGGCATCGAGGTCGTATGGACGAACACCCCGACGAA180
08.katG.Gene.MTB AACCGGTAAGGACGCGATCACCACCGGCATCGAGGTCGTATGGACGAACACCCCGACGAA180
*****
07.katG.Gene.MTB ATGGGACAAC190
10.katG.Gene.MTB ATGGGACAAC190
05.katG.Gene.MTB ATGGGACAAC190
04.katG.Gene.MTB ATGGGACAAC190
01.katG.Gene.MTB ATGGGACAAC190
02.katG.Gene.MTB ATGGGACAAC190
06.katG.Gene.MTB ATGGGACAAC190
09.katG.Gene.MTB ATGGGACAAC190
katG.gene.H37Rv ATGGGACAAC190
03.katG.Gene.MTB ATGGGACAAC190
08.katG.Gene.MTB ATGGGACAAC190
*****

```

Figure 2. Multiple alignments of mutated *katG* with H37Rv clarifying the mutations in our examined MDR-MTB strains including AGC→ACC (Ser→Thr) and AGC→CGC (Ser→Arg).

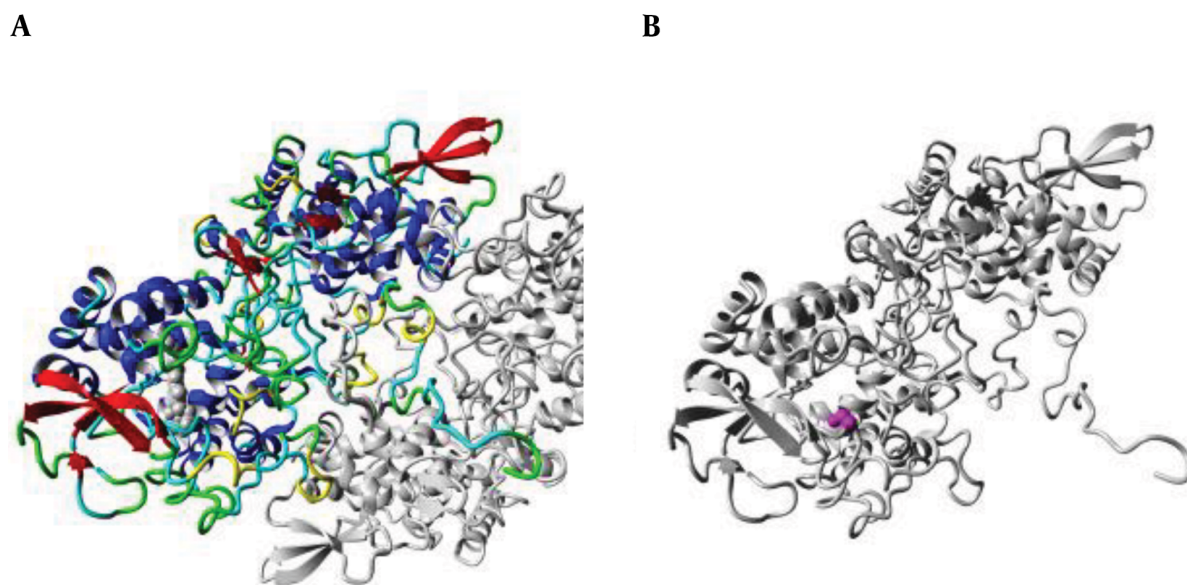


Figure 3. (A) An overview of the *KatG* protein in ribbon-presentation. The protein is colored by the element; α -helix = blue, β -strand = red, turn = green, 3/10 helix = yellow, and random coil = cyan. (B) The protein is colored grey, and the side chain of the mutated residue is colored magenta and shown as small balls. This shows the position of the mutation in the ribbon structure.

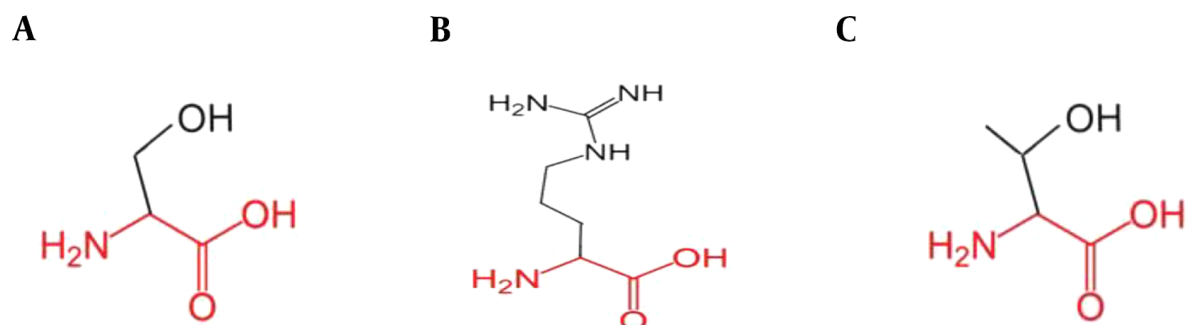


Figure 4. Schematic structures of (A) Serine (B) Arginine (C) Threonine.

Table 1. Energy Analysis of Receptor-Ligand Complex^a

TOS	TLRIE	LRVE	LREE	LRHE	LRSE	LRCE
1SJ2 wild-type- ISN	-3.80	-4.17	-0.81	-0.23	1.32	0.09
S315R-ISN	-5.18	-5.85	0.08	-0.23	0.72	0.09
S315T-ISN	-4.24	-5.28	0.14	0.00	0.82	0.09

Abbreviation: TOS, Type of structure; TLRIE, Total Ligand-Receptor Interaction Energy; LRVE, Ligand-Receptor Van der Waals Energy; LREE, Ligand-Receptor Electrostatic Energy; LRHE, Ligand-Receptor Hydrogen Bond Energy; LRSE, Ligand-Receptor Solvation Free Energy; LRCE Ligand-Receptor Conformational Entropy.

^a Energies are in Kcal/mol.

-3.80 kcal/mol, -4.24 kcal/mol, and -5.18 kcal/mol, respectively, as shown in Table 1. The low energy of the mutant

complex showed a strong binding affinity between mutant *M. tuberculosis KatG* and INH. Because of this tight binding,

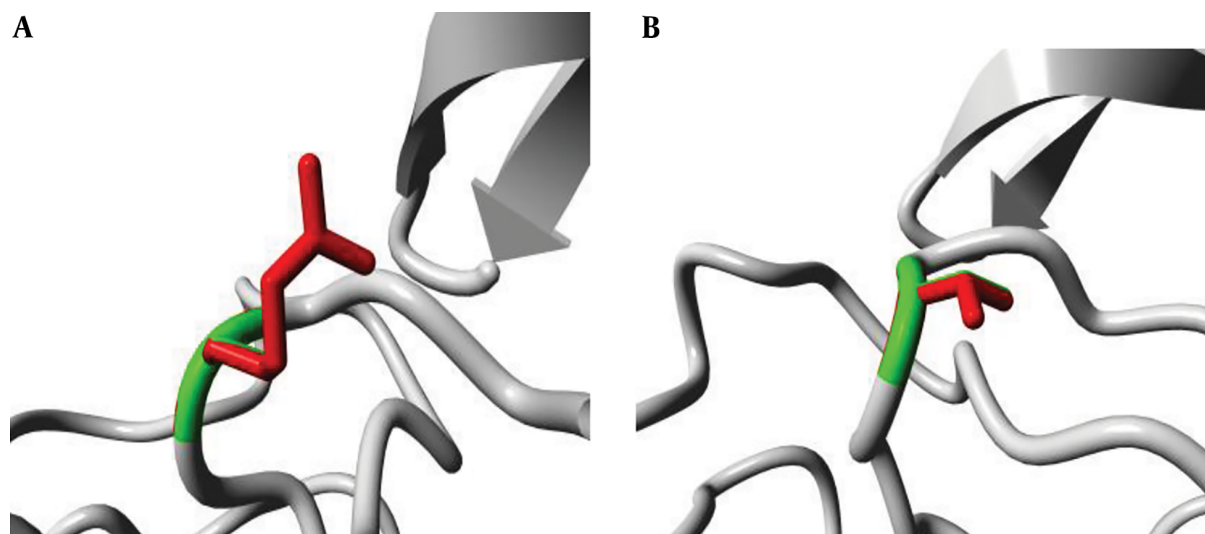


Figure 5. (A) Close view of mutation S315R, (B) Close view of mutation S315T. The protein is colored grey; the side chains of both wild-type and mutant residues are shown and colored green and red, respectively.

INH will lose the ability to convert itself into an active form (IN-NAD), which is significant for lethal action and staying unsusceptible to mutant *KatG*.

The bindings of mutant *KatG* residues were observed dissimilar to the wild type, as shown in Figure 7. There was only one hydrogen bond at Lys274 in the wild type and six hydrophobic interactions with residues Arg104, Pro232, Thr275, His276, Leu378, and Ser315. There was no hydrogen bond in mutant S315R *KatG*, having five hydrophobic interactions at positions Arg104, Trp107, His270, Trp321, and Arg315. Hydrogen bonds were observed distorted in mutant 315, and it is the only similar position between wild and mutant complexes. Furthermore, in mutant S315T, it was observed that a new residue of Asp137 interacted to INH through the hydrogen bond while two new residues of Trp321 and His270 were observed to participate in hydrophobic interactions.

Thus, His270, His276, and Ser315 were seemed to be key binding residues of this binding pocket and were observed to be involved in the drug-protein complex, as shown in Figure 6. Attractions among binding residues and structural arrangements were affected due to the difference in the size and hydrophobic properties of mutant amino acids. The most significant elements responsible for inactivation are changes in binding residues, as observed in the computational model. Indeed, the resistance mechanism against different drugs, including isoniazid is poorly understood. It has been found that different approaches and techniques are used to determine resistance mechanisms associated with mutations in MDR- tuberculosis (24).

This computational investigation showed that variations in binding residues and differences in docking energies due to mutations might be responsible for the inactivation of INH, leading to resistance in *M. tuberculosis* clinical isolates. Changes in the binding pattern and interacting residues would lose the ability of INH to convert itself into an active form (IN-NAD), which is significant for lethal action and staying unsusceptible to mutant *KatG*. It was concluded that isoniazid performs better when Ser is at position 315, and the mutation of Arg or Thr at the mentioned position significantly harms the enzyme function. This study will help researchers to better understand the mechanism of resistance development by the bacterium and confirms some of the previously reported results by other researchers. We hope that this data analysis will provide important knowledge relevant to drug resistance and the level of resistance in different MTB strains.

Footnotes

Authors' Contribution: Conceptualization: Muhammad Mumtaz Khan, Maria Silvana Alves, and Muhammad Jahangir; Methods: Muhammad Mumtaz Khan, Rehmat Zaman, Aisha Bibi, and Sajid Ali; Software: Muhammad Mumtaz Khan, Mustafa Kamal, and Abdul Jabbar; Writing: Muhammad Mumtaz Khan and Mohammad Haroon Khan; Data analysis and editing: Sadia Alam.

Conflict of Interests: The authors have no conflict of interest.

Funding/Support: No funding was received.

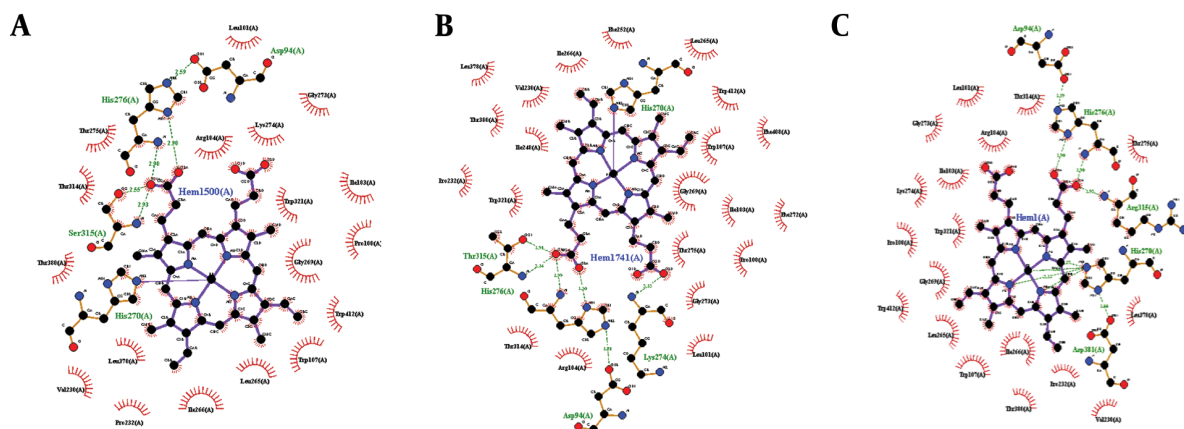


Figure 6. (A) Binding of 1S2 with heme; original binding of wild-type 1S2 was predicted through wet lab. The bonding pattern is as His270 = one covalent link, His276 = two H-bonds, and Ser315 = two H-bonds; (B) Binding of 1S2 Ser315Thr with heme. The bonding pattern is as His270 = one covalent link, His276 = two H-bonds, Thr315 = two H-bonds, and Lys274 = one H-bond; (C) Binding of 1S2 Ser315Arg with heme. The bonding pattern is as His270 = three H-bonds, His276 = two H-bonds, and Arg315 = one H-bond.

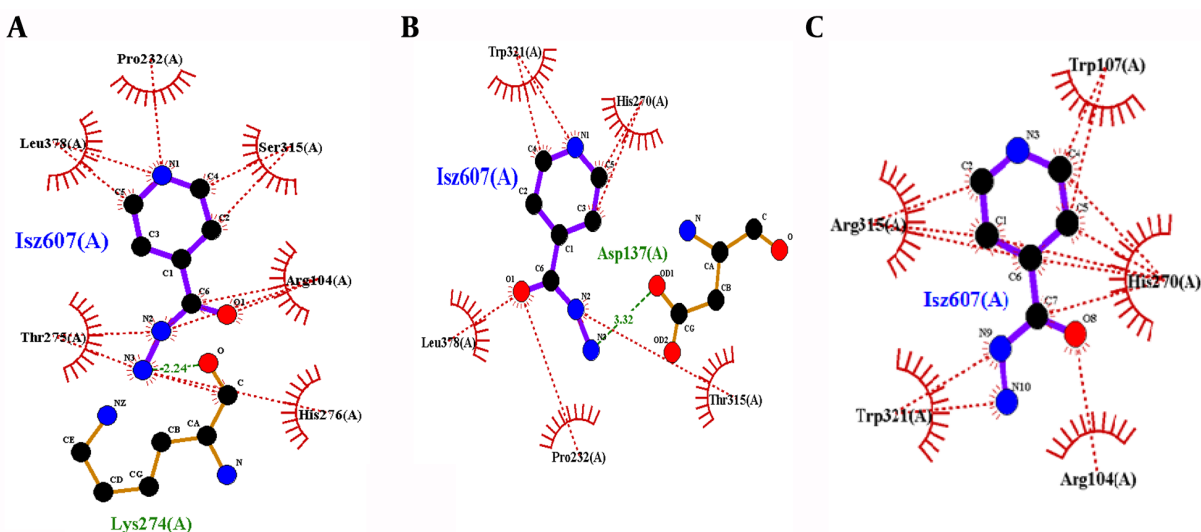


Figure 7. (A) Binding mode of INH with wild-type *KatG* (1S2) of *Mycobacterium tuberculosis*; (B) Binding mode of INH and S315T *KatG* of *Mycobacterium tuberculosis*.

Informed Consent: Informed consent was obtained from patients. Sputum samples of pulmonary tuberculosis patients were collected at the Ojha Institute of Chest Diseases (OICD), Dow University of Health Sciences, Karachi, Pakistan, after obtaining the patients' consent.

References

- Tostmann A, Kik SV, Kalisvaart NA, Sebek MM, Verver S, Boeree MJ, et al. Tuberculosis transmission by patients with smear-negative pulmonary tuberculosis in a large cohort in the Netherlands. *Clin Infect Dis*. 2008;**47**(9):1135–42. doi: [10.1086/591974](https://doi.org/10.1086/591974). [PubMed: [18823268](https://pubmed.ncbi.nlm.nih.gov/18823268/)].
- Lillebaek T, Norman A, Rasmussen EM, Marvig RL, Folkvardsen DB, Andersen AB, et al. Substantial molecular evolution and mutation rates in prolonged latent *Mycobacterium tuberculosis* infection in humans. *Int J Med Microbiol*. 2016;**306**(7):580–5. doi: [10.1016/j.ijmm.2016.05.017](https://doi.org/10.1016/j.ijmm.2016.05.017). [PubMed: [27296510](https://pubmed.ncbi.nlm.nih.gov/27296510/)].
- World Health Organisation. *Global tuberculosis report, executive summary*. 2019. Available from: <https://www.who.int/teams/global-tuberculosis-programme/tb-reports/global-report-2019>.
- Zhang Y, Yew WW. Mechanisms of drug resistance in *Mycobacterium tuberculosis*: update 2015. *Int J Tuberc Lung Dis*. 2015;**19**(11):1276–89. doi: [10.5588/ijtld.15.0389](https://doi.org/10.5588/ijtld.15.0389). [PubMed: [26467578](https://pubmed.ncbi.nlm.nih.gov/26467578/)].
- Iqbal S, Shabir I, Iqbal R, Riazudin S. Role of *katG* gene in resistant build up against isoniazid (INH)-A first line anti-TB drug. *Int J Agric Biol*. 2004;**6**(3):581–4.

6. Manson AL, Cohen KA, Abeel T, Desjardins CA, Armstrong DT, Barry C3, et al. Genomic analysis of globally diverse Mycobacterium tuberculosis strains provides insights into the emergence and spread of multidrug resistance. *Nat Genet.* 2017;**49**(3):395–402. doi: [10.1038/ng.3767](https://doi.org/10.1038/ng.3767). [PubMed: [28092681](https://pubmed.ncbi.nlm.nih.gov/28092681/)]. [PubMed Central: [PMC5402762](https://pubmed.ncbi.nlm.nih.gov/PMC5402762/)].
7. Miotto P, Piana F, Penati V, Canducci F, Migliori GB, Cirillo DM. Use of genotype MTBDR assay for molecular detection of rifampin and isoniazid resistance in Mycobacterium tuberculosis clinical strains isolated in Italy. *J Clin Microbiol.* 2006;**44**(7):2485–91. doi: [10.1128/JCM.00083-06](https://doi.org/10.1128/JCM.00083-06). [PubMed: [16825369](https://pubmed.ncbi.nlm.nih.gov/16825369/)]. [PubMed Central: [PMC1489497](https://pubmed.ncbi.nlm.nih.gov/PMC1489497/)].
8. Takawira FT, Mandishora RSD, Dhlamini Z, Munemo E, Stray-Pedersen B. Mutations in rpoB and katG genes of multidrug resistant Mycobacterium tuberculosis undetectable using genotyping diagnostic methods. *Pan Afr Med J.* 2017;**27**:145. doi: [10.11604/pamj.2017.27.145.10883](https://doi.org/10.11604/pamj.2017.27.145.10883). [PubMed: [28904673](https://pubmed.ncbi.nlm.nih.gov/28904673/)]. [PubMed Central: [PMC5567934](https://pubmed.ncbi.nlm.nih.gov/PMC5567934/)].
9. Bostanabad SZ, Titov LP, Bahrmand A, Nojoumi SA. Detection of mutation in isoniazid-resistant Mycobacterium tuberculosis isolates from tuberculosis patients in Belarus. *Indian J Med Microbiol.* 2008;**26**(2):143–7. doi: [10.4103/0255-0857.40528](https://doi.org/10.4103/0255-0857.40528). [PubMed: [18445950](https://pubmed.ncbi.nlm.nih.gov/18445950/)].
10. Unissa AN, Subbian S, Hanna LE, Selvakumar N. Overview on mechanisms of isoniazid action and resistance in Mycobacterium tuberculosis. *Infect Genet Evol.* 2016;**45**:474–92. doi: [10.1016/j.meegid.2016.09.004](https://doi.org/10.1016/j.meegid.2016.09.004). [PubMed: [27612406](https://pubmed.ncbi.nlm.nih.gov/27612406/)].
11. Mailaender C, Reiling N, Engelhardt H, Bossmann S, Ehlers S, Niederweis M. The MspA porin promotes growth and increases antibiotic susceptibility of both Mycobacterium bovis BCG and Mycobacterium tuberculosis. *Microbiology (Reading).* 2004;**150**(Pt 4):853–64. doi: [10.1099/mic.0.26902-0](https://doi.org/10.1099/mic.0.26902-0). [PubMed: [15073295](https://pubmed.ncbi.nlm.nih.gov/15073295/)].
12. Hameed HMA, Islam MM, Chhotaray C, Wang C, Liu Y, Tan Y, et al. Molecular targets related drug resistance mechanisms in MDR-, XDR-, and TDR-Mycobacterium tuberculosis Strains. *Front Cell Infect Microbiol.* 2018;**8**:114. doi: [10.3389/fcimb.2018.00114](https://doi.org/10.3389/fcimb.2018.00114). [PubMed: [29755957](https://pubmed.ncbi.nlm.nih.gov/29755957/)]. [PubMed Central: [PMC5932416](https://pubmed.ncbi.nlm.nih.gov/PMC5932416/)].
13. Ghiladi RA, Knudsen GM, Medzihradzky KF, Ortiz de Montellano PR. The Met-Tyr-Trp cross-link in Mycobacterium tuberculosis catalase-peroxidase (KatG): autocatalytic formation and effect on enzyme catalysis and spectroscopic properties. *J Biol Chem.* 2005;**280**(24):22651–63. doi: [10.1074/jbc.M502486200](https://doi.org/10.1074/jbc.M502486200). [PubMed: [15840564](https://pubmed.ncbi.nlm.nih.gov/15840564/)].
14. Shrestha R, Joshi RN, Joshi K, Poudel BH, Shrestha BG. Analysis of KatG Ser315Thr mutation in multidrug resistant Mycobacterium tuberculosis and SLC11A1 polymorphism in multidrug resistance tuberculosis in central development region of Nepal using PCR-RFLP technique: a pilot study. *Nepal J Biotechnol.* 2011;**1**(1):14–21.
15. Kapur V, Li LL, Iordanescu S, Hamrick MR, Wanger A, Kreiswirth BN, et al. Characterization by automated DNA sequencing of mutations in the gene (rpoB) encoding the RNA polymerase beta subunit in rifampin-resistant Mycobacterium tuberculosis strains from New York City and Texas. *J Clin Microbiol.* 1994;**32**(4):1095–8. doi: [10.1128/JCM.32.4.1095-1098.1994](https://doi.org/10.1128/JCM.32.4.1095-1098.1994). [PubMed: [8027320](https://pubmed.ncbi.nlm.nih.gov/8027320/)]. [PubMed Central: [PMC267194](https://pubmed.ncbi.nlm.nih.gov/PMC267194/)].
16. Solis FJ, Wets RJ. Minimization by random search techniques. *Math Oper Res.* 1981;**6**(1):19–30. doi: [10.1287/moor.6.1.19](https://doi.org/10.1287/moor.6.1.19).
17. Han LY, Lin HH, Li ZR, Zheng CJ, Cao ZW, Xie B, et al. PEARLS: program for energetic analysis of receptor-ligand system. *J Chem Inf Model.* 2006;**46**(1):445–50. doi: [10.1021/ci0502146](https://doi.org/10.1021/ci0502146). [PubMed: [16426079](https://pubmed.ncbi.nlm.nih.gov/16426079/)].
18. Parrish N, Osterhout G, Dionne K, Sweeney A, Kwiatkowski N, Carroll K, et al. Rapid, standardized method for determination of Mycobacterium tuberculosis drug susceptibility by use of mycolic acid analysis. *J Clin Microbiol.* 2007;**45**(12):3915–20. doi: [10.1128/JCM.02528-06](https://doi.org/10.1128/JCM.02528-06). [PubMed: [17913928](https://pubmed.ncbi.nlm.nih.gov/17913928/)]. [PubMed Central: [PMC2168583](https://pubmed.ncbi.nlm.nih.gov/PMC2168583/)].
19. Ali A, Hasan Z, Moatter T, Tanveer M, Hasan R. M. tuberculosis Central Asian Strain 1 MDR isolates have more mutations in rpoB and katG genes compared with other genotypes. *Scand J Infect Dis.* 2009;**41**(1):37–44. doi: [10.1080/00365540802570519](https://doi.org/10.1080/00365540802570519). [PubMed: [19012077](https://pubmed.ncbi.nlm.nih.gov/19012077/)].
20. Marti-Renom MA, Stuart AC, Fiser A, Sanchez R, Melo F, Sali A. Comparative protein structure modeling of genes and genomes. *Annu Rev Biophys Biomol Struct.* 2000;**29**:291–325. doi: [10.1146/annurev.biophys.29.1.291](https://doi.org/10.1146/annurev.biophys.29.1.291). [PubMed: [10940251](https://pubmed.ncbi.nlm.nih.gov/10940251/)].
21. Vriend G. WHAT IF: A molecular modeling and drug design program. *J Mol Graph.* 1990;**8**(1):52–6. doi: [10.1016/0263-7855\(90\)80070-v](https://doi.org/10.1016/0263-7855(90)80070-v).
22. Feldman HJ, Snyder KA, Ticol A, Pintilie G, Hogue CW. A complete small molecule dataset from the protein data bank. *FEBS Lett.* 2006;**580**(6):1649–53. doi: [10.1016/j.febslet.2006.02.003](https://doi.org/10.1016/j.febslet.2006.02.003). [PubMed: [16494871](https://pubmed.ncbi.nlm.nih.gov/16494871/)].
23. Morris GM, Huey R, Lindstrom W, Sanner MF, Belew RK, Goodsell DS, et al. AutoDock4 and AutoDockTools4: Automated docking with selective receptor flexibility. *J Comput Chem.* 2009;**30**(16):2785–91. doi: [10.1002/jcc.21256](https://doi.org/10.1002/jcc.21256). [PubMed: [19399780](https://pubmed.ncbi.nlm.nih.gov/19399780/)]. [PubMed Central: [PMC2760638](https://pubmed.ncbi.nlm.nih.gov/PMC2760638/)].
24. Venselaar H, Te Beek TA, Kuipers RK, Hekkelman ML, Vriend G. Protein structure analysis of mutations causing inheritable diseases. An e-Science approach with life scientist friendly interfaces. *BMC Bioinformatics.* 2010;**11**:548. doi: [10.1186/1471-2105-11-548](https://doi.org/10.1186/1471-2105-11-548). [PubMed: [21059217](https://pubmed.ncbi.nlm.nih.gov/21059217/)]. [PubMed Central: [PMC2992548](https://pubmed.ncbi.nlm.nih.gov/PMC2992548/)].
25. Yao C, Zhu T, Li Y, Zhang L, Zhang B, Huang J, et al. Detection of rpoB, katG and inhA gene mutations in Mycobacterium tuberculosis clinical isolates from Chongqing as determined by microarray. *Clin Microbiol Infect.* 2010;**16**(11):1639–43. doi: [10.1111/j.1469-0691.2010.03267.x](https://doi.org/10.1111/j.1469-0691.2010.03267.x). [PubMed: [20491829](https://pubmed.ncbi.nlm.nih.gov/20491829/)].
26. Wang JC, Lin JH. Scoring functions for prediction of protein-ligand interactions. *Curr Pharm Des.* 2013;**19**(12):2174–82. doi: [10.2174/1381612811319120005](https://doi.org/10.2174/1381612811319120005). [PubMed: [23016847](https://pubmed.ncbi.nlm.nih.gov/23016847/)].
27. Purohit R, Rajendran V, Sethumadhavan R. Relationship between mutation of serine residue at 315th position in M. tuberculosis catalase-peroxidase enzyme and Isoniazid susceptibility: an in silico analysis. *J Mol Model.* 2011;**17**(4):869–77. doi: [10.1007/s00894-010-0785-6](https://doi.org/10.1007/s00894-010-0785-6). [PubMed: [20593210](https://pubmed.ncbi.nlm.nih.gov/20593210/)].